4050–4058 *Nucleic Acids Research, 1999, Vol. 27, No. 20*

Topoisomerase III is essential for accurate nuclear division in *Schizosaccharomyces pombe*

Adele Goodwin[1], Shao-Win Wang[1,2], Takashi Toda[2], Chris Norbury[1] and Ian D. Hickson[1,*]

Imperial Cancer Research Fund Laboratories, [1]Institute of Molecular Medicine, University of Oxford, John Radcliffe Hospital, Oxford OX3 9DS, UK and [2]Cell Regulation Laboratory, 44 Lincoln's Inn Fields, London WC2A 3PX, UK

Received June 21, 1999; Revised and Accepted August 25, 1999

ABSTRACT

Topoisomerases catalyse changes in the topological state of DNA and are required for many aspects of DNA metabolism. While the functions of topoisomerases I and II in eukaryotes are well established, the role of topoisomerase III remains poorly defined. We have identified a gene in the fission yeast *Schizosaccharomyces pombe*, designated *top3*$^+$, which shows significant sequence similarity to genes encoding topoisomerase III enzymes in other eukaryotic species. In common with murine *TOP3*α, but in contrast to *Saccharomyces cerevisiae TOP3*, the *S.pombe top3*$^+$ gene is essential for long-term cell viability. Fission yeast haploid spores containing a disrupted *top3*$^+$ gene germinate successfully, but then undergo only a limited number of cell divisions. Analysis of these *top3* mutants revealed evidence of aberrant mitotic chromosome segregation, including the 'cut' phenotype, where septation is completed prior to nuclear division. Consistent with the existence of an intimate association (originally identified in *S.cerevisiae*) between topoisomerase III and DNA helicases of the RecQ family, deletion of the *rqh1*$^+$ gene encoding the only known RecQ helicase in *S.pombe* suppresses lethality in *top3* mutants. This conservation of genetic interaction between two widely diverged yeasts suggests that the RecQ family helicases encoded by the Bloom's and Werner's syndrome genes are likely to act in concert with topoisomerase III isozymes in human cells. Our data are consistent with a model in which the association of a RecQ helicase and topoisomerase III is important for facilitating decatenation of late stage replicons to permit faithful chromosome segregation during anaphase.

INTRODUCTION

Topoisomerases are ubiquitous nuclear enzymes required for many aspects of DNA metabolism in both prokaryotes and eukaryotes (reviewed in 1,2). Topoisomerases catalyse changes in the topological state of DNA through their ability to cleave the DNA backbone and pass intact DNA strands through the break. There are two classes of topoisomerase enzymes, designated types I and II; the former create single-stranded breaks and the latter double-stranded breaks in DNA. One member of the type I class in eukaryotes is topoisomerase (topo) III, an enzyme that shares sequence and mechanistic similarity with bacterial topo I and III. These so-called type IA enzymes make a transient covalent linkage to the 5′-end of the cleaved DNA during their catalytic cycle and catalyse relaxation only of negatively supercoiled DNA (1,2).

The best characterised eukaryotic topo III enzyme is from the budding yeast *Saccharomyces cerevisiae*. In this organism, *top3*Δ mutants are viable, but show hyper-recombination in repetitive DNA sequences and an extended cell cycle transit time characterised by an accumulation of cells in the late S/G_2 phases (3,4). This slow growth phenotype can be suppressed by loss of function mutations in the *SGS1* gene (4), encoding a DNA helicase belonging to the RecQ family (reviewed in 5). This family has attracted considerable attention recently with the finding that the genes mutated in the human Bloom's and Werner's syndromes encode RecQ family members (6,7). These rare genetic disorders are characterised by an elevated incidence of cancers and premature ageing, respectively (reviewed in 8–10). In common with *S.cerevisiae top3* mutants, cells derived from Bloom's and Werner's syndrome individuals display genomic instability; excessive sister chromatid exchanges in the case of Bloom's cells and large chromosomal deletions in Werner's cells (11,12).

To date, two topo III isozymes have been identified in mammalian cells. The *hTOP3*α gene is located on human chromosome 17p11.2–12 (13) and its mouse counterpart has been shown to be essential for embryonic development (14). A potentially interesting connection between *hTOP3*α and the cancer predisposition disorder ataxia telangiectasia (AT) has been suggested by the observation that overexpression of a truncated version of topo IIIα influences cell cycle and apoptotic responses to ionising radiation in AT cells (15). Recently, a second human topo III gene, *hTOP3*β, was discovered through sequencing of genomic DNA around the immunoglobulin λ locus on chromosome 22q11 (16). This new gene produces three alternatively spliced transcripts encoding proteins differing in their C-terminal DNA binding domains. Topo IIIβ can partially substitute for *S.cerevisiae* topo III and has been shown to interact physically with Sgs1p using both two-hybrid and co-immunoprecipitation methods (17).

Although *S.cerevisiae top3* mutants have been partially characterised, the biochemical basis of the most striking

*To whom correspondence should be addressed. Tel: +44 1865 222417; Fax: +44 1865 222431; Email: hickson@icrf.icnet.uk

phenotypic consequence of loss of topo III function, namely severely slowed growth (3,4), remains unresolved. Moreover, any analysis of budding yeast *top3* mutants is hampered by the rapid emergence of extragenic mutations (usually in *SGS1*) which suppress the slow growth phenotype (4). Hence, we sought an alternative, genetically amenable, model system for analysis of the functions of this important enzyme. Using data emerging from the *Schizosaccharomyces pombe* genome sequencing project, we identified sequences showing significant similiarity to *TOP3* genes from other eukaryotic organisms. Here, we show that *S.pombe* topo III is essential for chromosome segregation during mitosis. Moreover, the lethality resulting from *top3*$^+$ gene disruption can be suppressed by mutation of the *rqh1*$^+$ gene (also called *rad12*$^+$ and *hus2*$^+$) (18–20), which encodes a yeast homologue of the human Bloom's and Werner's syndrome genes.

MATERIALS AND METHODS

Schizosaccharomyces pombe strains and methods

The genotypes of *S.pombe* strains used in this study are given in Table 1. Standard procedures for fission yeast genetics were followed, as described by Moreno *et al*. (21).

Identification of the *S.pombe top3*$^+$ gene

The *top3*$^+$ gene sequence was identified by BLAST searches of the Sanger Centre *S.pombe* genome database with the *S.cerevisiae* topo III protein sequence (3). This identified a sequence on chromosome II cosmid c16G5, NCBI accession no. CAA19038 (EMBL locus SPBC16G5, accession no. AL023554.1). Sequence alignments of the predicted *S.pombe top3*$^+$ gene product with other DNA topo III homologues were carried out using the DNASTAR Megalign program. Sequence comparisons with other DNA topos were performed using the Blast 2 Sequences program (blastp 2.0.9, matrix O BLOSUM 62). The M_r was calculated using the ExPASy Compute pI/MW tool (www.expasy.ch/tools/pI_tool.html).

Construction of a *top3* deletion mutant

The complete *ura4*$^+$ gene with 80 nt of flanking 5′ and 3′ *top3*$^+$ nucleotide sequence was amplified using PCR. The PCR primers for generation of the targeting fragment were as follows (written 5′→3′ with *top3*$^+$ sequences in bold): 5′ primer, **GCCATCTCGACCTTAACACCTTACACGCGAATTTTACACTGCAGTCATTTTTAAAAAAGGGAGATATAATTAGAAGGTGT**AAATCCCACTGGCTATATGT; 3′ primer, **AGGTAATAAGTTAATAAAAGTATACGAGCGGTCTGGTTATCTAGGTTTGCGGTTCATTATGACTCATAAGGTAGACTCTG**AATTCTAAATGCCTTCTGAC. The PCR-amplified fragment was precipitated and transformed using a LiAc/TE protocol based on the method of Keeney and Boeke (22) into the wild-type diploid strain CHP428/CHP429 (Table 1). Stable *ura*$^+$ colonies were picked and genomic DNA was isolated. Deletion of one copy of the *top3*$^+$ gene by homologous integration of the *ura4*$^+$ gene was confirmed using PCR. The heterozygous *top3*$^+$/*top3*::*ura4*$^+$ diploid (AG8sp) was then sporulated on malt extract agar, and tetrads were dissected onto YE5S agar. The spores were left to germinate at 30°C for 3–4 days.

Construction of *rqh1 top3* double mutant strains

The entire open reading frame of one allele of the *rqh1*$^+$ gene (18) in the *top3*$^+$/*top3*::*ura4*$^+$ diploid (AG8sp) was deleted by targeted integration of the *kanMX6* module according to the method of Bähler *et al*. (23). The PCR primers for generation of the targeting fragment were as follows (written 5′→3′ with *rqh1*$^+$ sequences in bold): 5′ primer, **GCAATTTGTGATTTTAGTTTTGCATTTCAACAGAACAATGCTTGGATGAGAACTCCTTAATTGCGGCTGTTGGAATTGGAAT**CGGATCCCCGGGTTAATTAA; 3′ primer, **GCCTACTTTCTAACGTATTATAGACAATGTTTAAATGAACGCACATGTACAATAAACGAACCATAAATTAACAGGAATAAA**ATCGATGAATTCGAGCTCG. Integration of the *kanMX6* module conferred G418 resistance to the transformed *top3*$^+$/*top3*::*ura4*$^+$ diploid (18,24). The *rqh1*::*kanMX6* deletion was confirmed by PCR, and the diploid (AG12sp) was sporulated and dissected as described above. Haploid colonies were replica plated to minimal agar plates lacking uracil and to YE plates containing 200 μg/ml G418 to select *top3*::*ura4*$^+$ and *rqh1*::*kanMX6* haploids, respectively.

top3$^+$ was also deleted in another *rqh1* mutant background (*rqh1-h2*). The targeting fragment for insertion of *kanMX6* into *top3*$^+$ was generated by PCR using the following primers (written 5′→3′ with the *top3*$^+$ sequences in bold): 5′ primer, **GCCATCTCGACCTTAACACCTTACACGCGAATTTTACACTGCAGTCATTTTTAAAAAAGGGAGATATAATTAGAAGGTGT**CGGATCCCCGGGTTAATTAA; 3′ primer, **AGGTAATAAGTTAATAAAAGTATACGAGCGGTCTGGTTATCTAGGTTTGCGGTTCATTATGACTCATAAGGTAGACTCTG**ATCGATGAATTCGAGCTCG.

Table 1. Yeast strains and plasmids

	Genotype	Reference
Strain		
CHP428/CHP429	*h*$^+$/*h*$^-$ *leu1-32*/*leu1-32 ura4-D18*/*ura4-D18 his7*/*his7 ade6-210*/*ade6-216*	Laboratory stock
AG8sp	*h*$^+$/*h*$^-$ *leu1-32*/*leu1-32 ura4-D18*/*ura4-D18 his7*/*his7 ade6-210*/*ade6-216 top3*$^+$/*top3*::*ura4*$^+$	This study
AG12sp	*h*$^+$/*h*$^-$ *leu1-32*/*leu1-32 ura4-D18*/*ura4-D18 his7*/*his7 ade6-210*/*ade6-216 top3*$^+$/*top3*::*ura4*$^+$ *rqh1*$^+$/*rqh1*::*kanMX6*	This study
rqh1-h2	*h*$^-$ *leu1-32 rqh1-h2*	P. Nurse
AG2sp	*h*$^-$ *leu1-32 rqh1-h2 top3*::*kanMX6*	This study
Plasmid		
pFA6a-kanMX6		J. Bähler

Nuclear staining of *top3* mutants

To analyse the nuclear DNA of *top3*::*ura4*$^+$ cells, the *top3*$^+$/*top3*::*ura4*$^+$ diploid (AG8sp) was allowed to sporulate and the resulting tetrads were dissected onto YE5S agar. After 2–3 days growth at 30°C, the *top3*::*ura4*$^+$ cells were lifted off the agar into 10 µl sterile H_2O. The cells were then fixed in 70% ethanol and mounted in Vectashield® mounting medium (Vector Laboratories) containing 1.5 µg/ml 4,6-diamidino-2-phenylindole (DAPI). The DNA was then visualised by fluorescence microsopy using a Zeiss Axioskop microscope and images captured using KromaScan software (Kinetic Imaging Ltd).

Analysis of growth rates

Cells were grown at 30°C in rich YE5S medium to mid log phase (10^6–10^7 cells/ml). The number of cells in each sample was determined using a semi-automated microcell counter (Sysmex F-820) and cultures were set up in YE5S medium at 10^6 cells/ml. The growth rates at 30°C were then monitored in duplicate by removing aliquots at intervals, and the cell numbers were counted as described above. The data were analysed and graphs were plotted in GraphPad Prism.

Flow cytometry

Mid log phase cells were fixed at a density of 10^7 cells/ml in 70% ethanol for 16 h at 4°C. Fixed cells were washed once in 50 mM sodium citrate (pH 7.0), resuspended in the same buffer containing 100 µg/ml DNase-free RNase A and incubated at 37°C for 4 h. Cells were then stained with 4 µg/ml propidium iodide, sonicated briefly and analysed by flow cytometry (FACScan; Becton Dickinson) using a 488 nm laser. Red fluorescence (DNA) and forward light scatter (cell size) data were collected for 10 000 cells for each sample. Data were analysed using CELLQuest software.

Analysis of hydroxyurea and UV responses

Segregants representing *top3*$^+$ *rqh1*$^+$ cells, the *rqh1*::*kanMX6* mutant, and the *top3*::*ura4*$^+$ *rqh1*::*kanMX6* double mutant were isolated from the dissected *top3*$^+$/*top3*::*ura4*$^+$ *rqh1*$^+$/*rqh1*::*kanMX6* heterozygous diploid (AG12sp). Cells were then grown in YE5S medium to mid log phase (10^6–10^7 cells/ml). The number of cells in each sample was counted using a haemacytometer, and cultures were standardized at 10^6 cells/ml. UV responses were then analysed by plating ~500 cells onto YE5S agar (in triplicate) and irradiating with 254 nm UV light in the dose range 0–200 J/m^2. Following irradiation, plates were incubated at 30°C for 3 days, after which the percentage of viable colonies in the UV-treated samples was calculated by comparison to the number of viable colonies in the untreated controls. Responses to hydroxyurea (HU) were tested by adding HU to a final concentration of 10 mM to liquid cultures. Samples were then taken at various times and plated (~500 cells) onto YE5S agar. The plates were incubated at 30°C for 3 days, before calculating the percentage of viable colonies, as described above. Data were analysed using Microsoft Excel and graphs plotted in GraphPad Prism. HU-treated cells were also fixed in 70% ethanol for each time point analysed. The DNA from these cells was then stained with DAPI and visualised as described above.

RESULTS

Cloning of the *S.pombe top3*$^+$ gene encoding topo III

The amino acid sequence of the *S.cerevisiae* topo III protein (3) was used to screen the partial *S.pombe* genome database held at the Sanger Centre. This comparison identified sequences on cosmid c16G5 from chromosome II that would encode a protein with strong sequence similarity to topo III. Through comparisons of this cosmid-encoded sequence with those of the budding yeast and human topo III proteins, together with predictions of the positions of splice donor and acceptor sites, the complete intron–exon structure of this gene, which we have designated *top3*$^+$, was compiled. Our predicted structure for the *top3*$^+$ gene matches that in the Sanger Centre database (NCBI accession no. CAA19038). The *top3*$^+$ gene is 2203 bp in length (from the translation start site to the TAG stop codon) and comprises six exons. All of the proposed splice donor and acceptor sequences match the *S.pombe* consensus.

The *top3*$^+$ mRNA would encode a protein comprising 622 amino acids with a calculated M_r of 71 169. Figure 1 shows an alignment of the predicted *S.pombe* topo III (Top3^{sp}) amino acid sequence with those of *S.cerevisiae* topo III, the human topo IIIα and β isozymes, and *Escherichia coli* topo I. Strong sequence similarity between the Top3^{sp} sequence and the predicted sequences of topo III proteins from the other species is evident throughout the length of Top3^{sp}. Percent identities and similarities in each case are given in the legend to Figure 1. The predicted active site residue of Top3^{sp} is Tyr330, through which the enzyme would make a transient covalent linkage to the 5′ phosphoryl group of the cleaved DNA.

The *top3*$^+$ gene is essential for long-term growth

To analyse the phenotype of fission yeast deficient in *top3*$^+$ function, a diploid strain (AG8sp) was generated in which one copy of the *top3*$^+$ gene was disrupted by insertion of the *ura4*$^+$ gene (see Materials and Methods). This heterozygous diploid strain was sporulated, and the resulting tetrads were dissected onto YE5S agar. Figure 2a shows that only two out of the four spores from each tetrad formed colonies visible to the naked eye. Replica plating of these haploid colonies onto medium lacking uracil indicated that the viable spores were exclusively ura$^-$, demonstrating that *top3*$^+$ is an essential gene.

Microscopic analysis of the dissected spores indicated that the *top3*::*ura4*$^+$ spores germinated successfully, but either failed to execute the first cell division (~14% of the germinated ura$^+$ spores) or underwent only a few rounds of cell division to form a microcolony. After 3 days of growth at 30°C, most of the microcolonies comprised ~30 cells, indicating that approximately five cell divisions had occurred following germination. After 7 days incubation, a small fraction of the microcolonies comprised 100–200 cells, but these cells were generally highly elongated, indicative of cell cycle arrest (Fig. 2b). These data suggest that death is a stochastic process in *S.pombe top3* mutants.

Chromosome segregation is abnormal in *top3* mutants

Given the role of topoisomerases in DNA replication and chromosome segregation, the gross nuclear structure in the *top3*::*ura4*$^+$ microcolonies was analysed using fluorescence microscopy of DAPI stained cells. To identify abnormal events

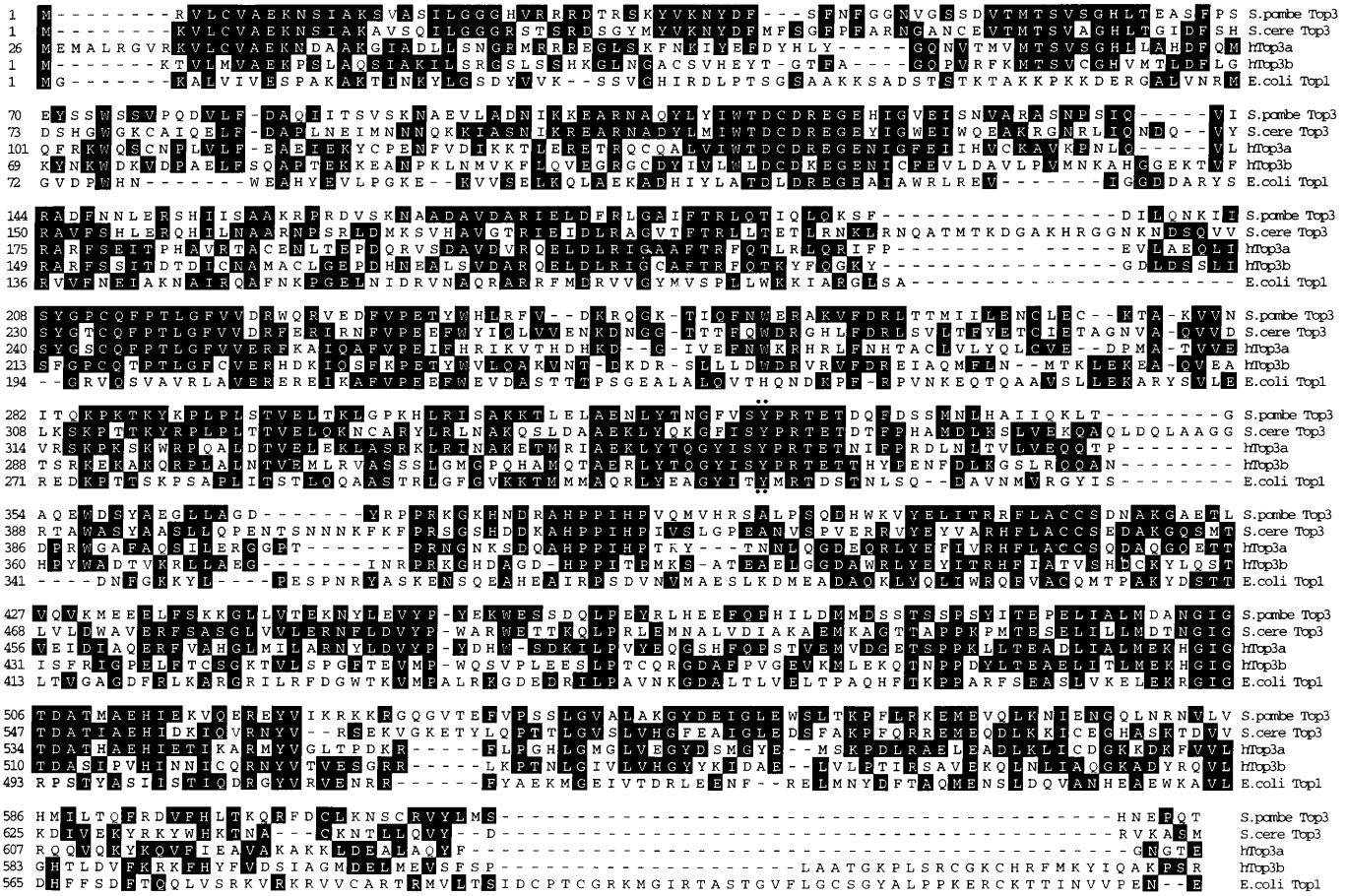

Figure 1. The *S.pombe top3*$^{+}$ gene. Alignment of the predicted amino acid sequences of *S.pombe* topo III with those of *S.cerevisiae* topo III, human topo IIIα (residues 26–640), human topo IIIβ (residues 1–640) and *E.coli* topo I (residues 1–640). Identical residues are indicated by black boxes. The putative active site tyrosine of *S.pombe* Top3^{sp} (Tyr330) is indicated by double dots above and below. Percent identities/similarities between the sequence of *S.pombe* Top3^{sp} and those of *S.cerevisiae* Top3p, human Top3α, human Top3β and *E.coli* topo I are, respectively, 44/60, 42/63, 33/51 and 24/42%.

occurring both at high frequency and in the first few rounds of cell division following germination, colonies were analysed at the earliest time point (48 h after dissection) that permitted unequivocal identification of the *top3*::*ura4*$^{+}$ spores. These analyses revealed a variety of nuclear defects in *top3*::*ura4*$^{+}$ cells indicative of a failure to execute faithful nuclear division (Fig. 3). Included amongst these defects were the 'cut' phenotype, where septation occurs in the absence of chromosome segregation and/or abnormal positioning of the nuclear DNA (top and middle panels), as well as extensive nuclear DNA fragmentation (bottom panel). Table 2 shows a compilation of the frequencies of the major nuclear DNA abnormalities observed in *top3*::*ura4* cells. In addition to these abnormalities, many of the mutant cells displayed gross morphological changes, being highly elongated and/or exhibiting evidence of extensive vacuolation. Such abnormalities are frequently seen in cell cycle mutants of *S.pombe*, secondary to earlier arrest of the nuclear cycle in cells with otherwise normal morphology. Hence, we consider it likely that such cells are displaying a relatively late stage, secondary phenotype.

The lethal phenotype of *top3* mutants is suppressed by disruption of *rqh*$^{+1}$

In budding yeast, the slow growth phenotype of *top3* mutants can be suppressed by loss of function mutations in the *SGS1* gene (4). Sgs1p is the sole member of the RecQ family of DNA helicases in budding yeast (reviewed in 5). We analysed, therefore, whether this genetic interaction between topo III and a RecQ helicase is conserved in the distantly related fission yeast. To this end, a diploid strain (AG12sp) was generated which is heterozygous for both *top3* and *rqh1*, the latter encoding the only RecQ family helicase currently identified in *S.pombe* (18–20). When tetrads resulting from sporulation of this diploid strain were dissected onto YE5S agar, ~75% of the spores produced viable colonies (Fig. 4a). Analysis of the genotypes of these haploid colonies by replica plating onto agar either lacking uracil, or containing G418, indicated that virtually all of the *top3 rqh1* double mutants were viable. These analyses also confirmed previous work indicating that *rqh1* single mutants are viable (18–20). The growth rate of *top3 rqh1* double mutants in both liquid and solid media was similar to that of

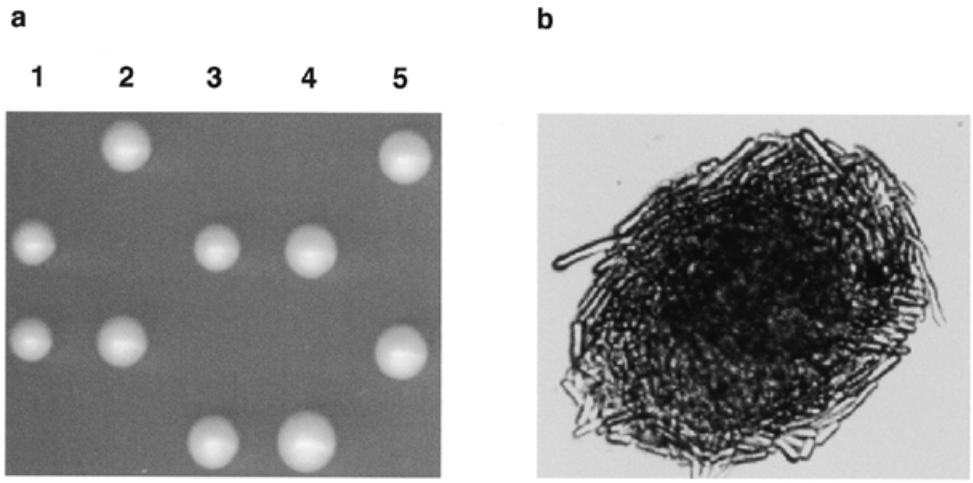

Figure 2. *Schizosaccharomyces pombe top3*$^+$ is an essential gene. (**a**) Haploid colonies resulting from dissection of *top3*$^+$/*top3*::*ura4*$^+$ heterozygous diploid (AG8sp) tetrads onto YE5S agar. Note the presence of only two visible colonies in each case. (**b**) Phase contrast image of a *top3*::*ura4*$^+$ microcolony after growth on YE5S agar for 7 days at 30°C.

Table 2. Nuclear abnormalities in *top3* mutants

Description of phenotype	Diagrammatic representation of phenotype	% cells with given phenotype
Wild-type		9.7%
'Cut'	or	19.3%
Single nucleus off centre (no septum)		27.3%
Aberrant segregation of nuclear DNA	or	11.3%
Fragmented nuclear DNA		16%
Elongated cell		8.4%
Elongated nucleus		4.6%

The remaining 3.4% represent aberrant cells that do not fit into any of the above categories. A total of 238 cells were analysed.

top3$^+$ *rqh1*$^+$ controls (Fig. 4b and c). We conclude that disruption of *rqh1*$^+$ suppresses the lethality conferred by loss of topo III function in *S.pombe*. We next asked whether a known mutant allele of *rqh1* (*rqh1-h2*) could also suppress lethality in *top3* mutants. Figure 4b shows that the AG2sp (*top3*::*kanMX6 rqh1-h2*) double mutant was viable and had a growth rate similar to that of a *top3 rqh1* double mutant in which the *rqh1*$^+$ gene is deleted. To analyse whether the cell cycle distribution of *rqh1 top3* double mutants was perturbed, flow cytometry was performed. Figure 5 shows that the vast majority of exponentially growing *rqh1 top3* mutant cells, like wild-type *S.pombe* cells and the *rqh1* mutant, are in the G_2 phase, suggesting that loss of both Rqh1p and Top3^{sp} does not obviously perturb cell cycle progression. Taken together, these data indicate that mutations in the *rqh1*$^+$ gene bypass the requirement for the essential *top3*$^+$ gene.

Response of *top3 rqh1* double mutants to DNA damaging agents and replication inhibitors

It has been shown previously that *S.pombe rqh1* mutants are sensitive both to UV light and to the ribonucleotide reductase inhibitor HU (18–20). The relative sensitivity of *top3*$^+$ *rqh1*$^+$, *rqh1* and *rqh1 top3* strains to these agents was therefore analysed in order to determine whether disruption of *top3*$^+$ could either suppress or exacerbate the sensitivity of an *rqh1* mutant to these agents. Figure 6 shows that the level of sensitivity of the *rqh1 top3* double mutant was comparable to that of a *rqh1* mutant.

DISCUSSION

We have identified a gene in the fission yeast *S.pombe* that shows a high degree of sequence similarity to genes encoding topo III enzymes from budding yeast and mammalian sources. The *S.pombe top3*$^+$ gene lies on chromosome II between two uncharacterised open reading frames (SPBC16G5.11c and SPBC16G5.13).

The phenotypes of *top3* mutants from fission yeast and budding yeast show similarities and differences. In each case, mutants show impaired growth and viability, but in the case of *S.pombe top3* this deficit results in lethality, whereas in budding yeast it does not (3,4; this work). However, in both cases near normal viability can be restored by inactivating the only known RecQ family helicase gene found in each organism (4; this work). Although there is no evidence that

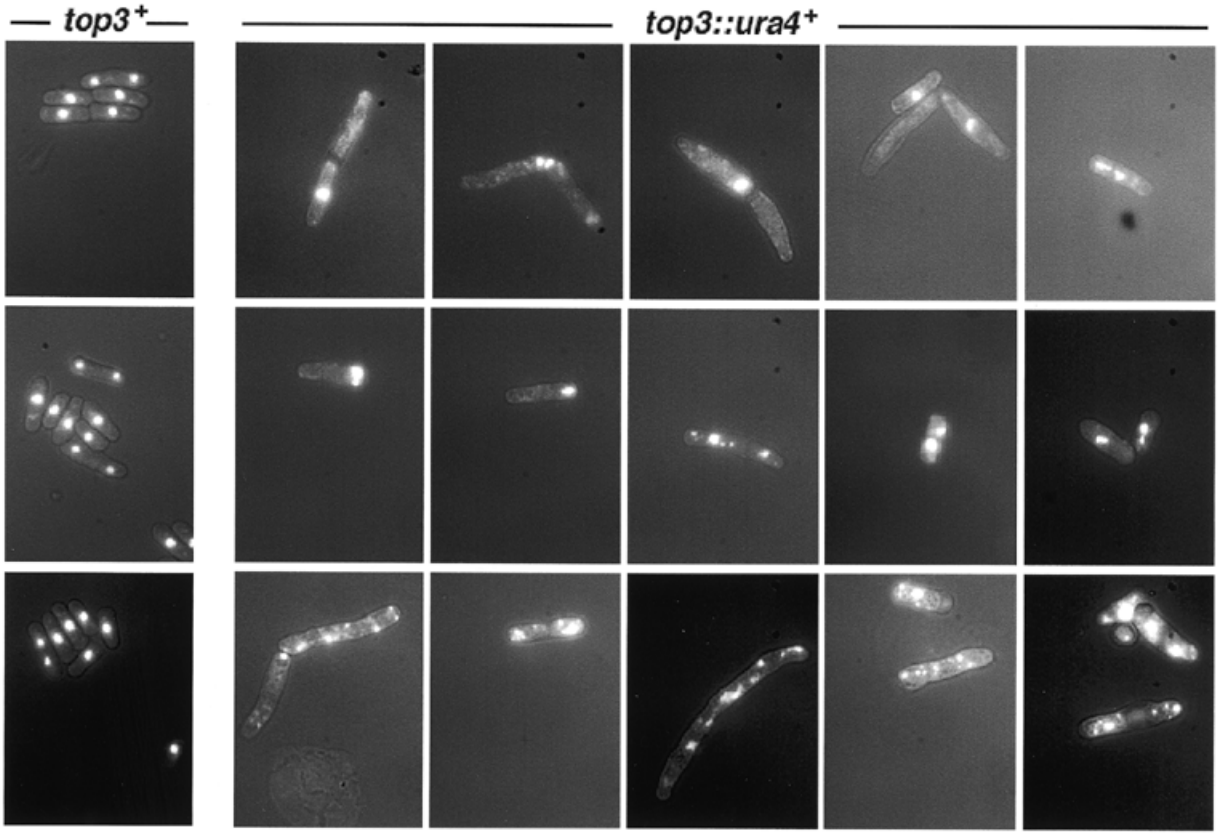

Figure 3. Fluorescence microscopy of DAPI-stained *top3*::*ura4*$^+$ cells. Examples of *top3*::*ura4*$^+$ cells or *top3*$^+$ controls (as indicated above the panels) stained with DAPI to indicate the location of nuclear DNA. Examples of the 'cut' phenotype and/or abnormal positioning/unequal partitioning of nuclear DNA (upper and middle rows), and nuclear fragmentation (lower row) are shown for the *top3*::*ura4*$^+$ cells.

S.cerevisiae top3 mutants exhibit a defect in nuclear division, to our knowledge there have not been any data published to date that address this issue directly. What is clear, however, is that *S.cerevisiae top3* mutants fail to execute the transition from late S phase into anaphase with the proper kinetics (3,4), perhaps indicating that these mutants also experience difficulty in segregating newly replicated sister chromatids.

There is a striking similarity between the phenotypes of fission yeast mutants lacking topo II and those lacking topo III, suggesting that these two mechanistically dissimilar enzymes nevertheless participate in the same general process(es). In common with *top3* mutants, *top2* mutants die during aberrant mitosis in which nuclear DNA is unevenly segregated between the daughter cells (25,26). These mutants also demonstrate the 'cut' phenotype, whereby cell division is not coordinated with nuclear division (25,26).

In budding yeast, mutations in *TOP3* confer a severe slow growth phenotype that is suppressed rapidly upon continuous culture of the mutant, generally by mutation of *SGS1* (4). In contrast, we found no evidence for the rapid emergence of similar extragenic suppressor mutations (such as *rqh1*) during the limited proliferative phase of the dissected *S.pombe top3*::*ura4*$^+$ colonies. We consider it likely that this reflects the relatively small number of cell divisions that *S.pombe top3* mutants undergo prior to death. When constructed by gene disruption, *S.pombe top3 rqh1* double mutants show only a modest growth deficit (Fig. 4c) and fluorescence microscopy of DAPI stained cells indicates that they execute apparently normal mitoses (data not shown). Moreover, the phenotypic characteristics of the double mutant in terms of UV and HU sensitivity (Fig. 6), and of exhibiting 'cut' cells only ~8 h after exposure to HU (data not shown) are indistinguishable from those of a *rqh1* mutant (18).

The underlying mechanism by which deletion of genes encoding RecQ helicases suppresses growth defects in *top3* mutants is not known at this stage. Based on previous data from analysis of budding yeast mutants (4), and on the model discussed below, we would place Rqh1 upstream of Top3^{sp} in the biochemical pathway leading to faithful chromosome segregation. Hence, we would suggest that the helicase action of Rqh1 generates a substrate for Top3^{sp} and that in the absence of Top3^{sp} this as yet unidentified DNA structure is toxic. However, in the absence of both Rqh1 and Top3^{sp}, the toxic structure does not arise. Clearly an alternative route for dealing with the problems inherent in segregating intertwined chromosomes must exist in *rqh1 top3* double mutants. This is likely to

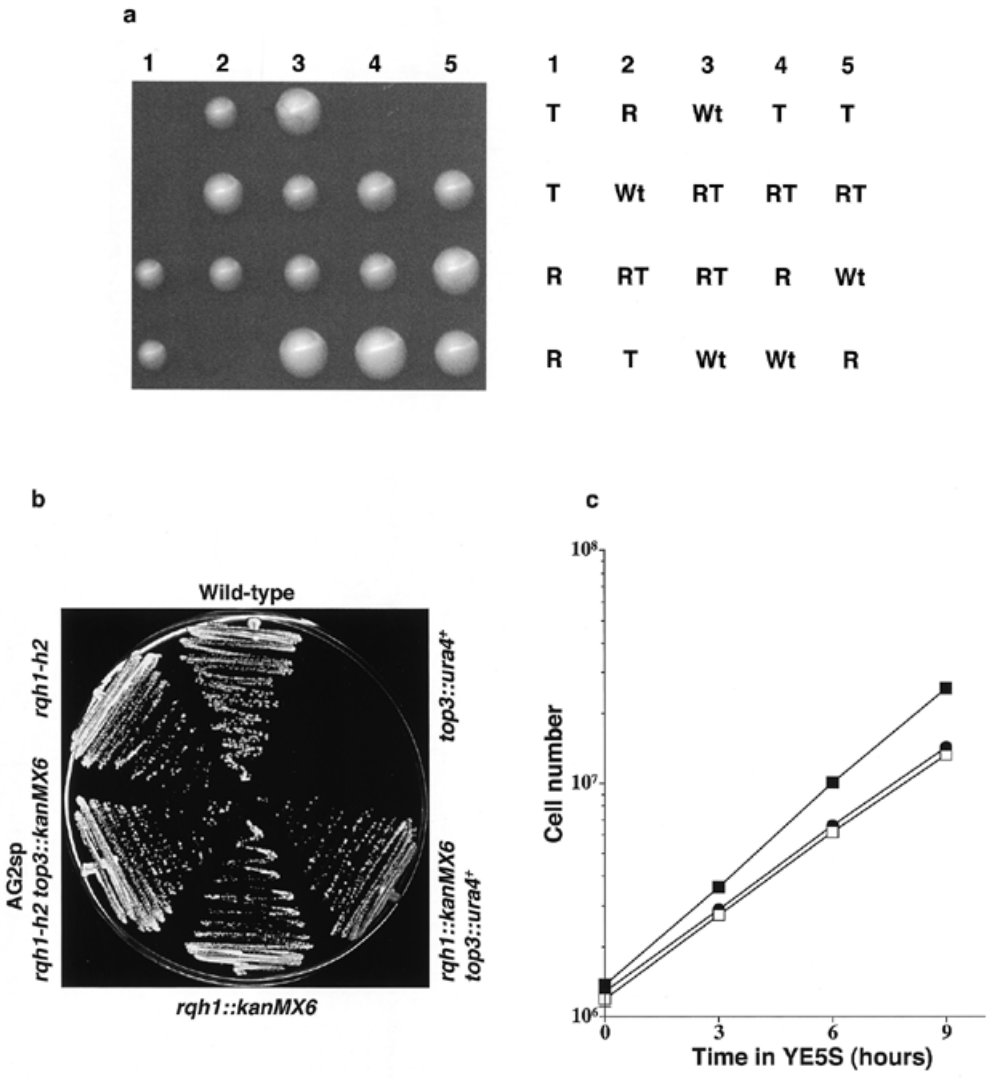

Figure 4. Disruption of *rqh1*$^+$ suppresses lethality of *top3* mutants. (**a**) Haploid colonies resulting from dissection of five AG12sp tetrads onto YE5S agar. The genotypes of the colonies are indicated on the right. Wt, wild-type (i.e. *top3*$^+$ *rqh1*$^+$); T, *top3*::*ura4*$^+$; R, *rqh1*::*kanMX6*; RT, *top3*::*ura4*$^+$ *rqh1*::*kanMX6*. (**b**) Examples of cells with the four genotypes indicated in (a), together with a *rqh1-h2* mutant and the AG2sp double mutant (*top3*::*kanMX6 rqh1-h2*) were streaked onto YE5S agar. The *top3*::*ura4*$^+$ sample was included as a control in (b), however, the inoculum was necessarily much lower than for the other samples. Nevertheless, no visible colonies were ever derived from re-streaking the *top3*::*ura4*$^+$ microcolonies in this way. (**c**) Growth curves of exponentially growing cultures of wild-type (i.e. *top3*$^+$ *rqh1*$^+$) (filled square), *rqh1*::*kanMX6* (open square) and *rqh1*::*kanMX6 top3*::*ura4*$^+$ (filled circle) strains.

involve the double-stranded DNA decatenation pathway dependent upon topo II protein (1,2). Thus, it is possible that *rqh1 top3* double mutants show a greater dependency than do wild-type cells on efficient topo II function. This hypothesis can be tested by analysis of the effects of deleting *rqh1*$^+$ and *top3*$^+$ in mutants encoding temperature-sensitive topo II enzymes.

We and others have previously proposed that the primary topological challenge leading to cell death in topo-deficient mutants is a result of the difficulties inherent in replicating the portion of chromosomes where replication forks converge (27,28). In this model, steric and/or topological constraints prevent the replication machinery from completing duplication of the last portion of each replicon. One solution to this problem is for a helicase (such as Rqh1) to unwind the unreplicated duplex, thereby converting the supercoiling of the helix into catenation (intertwining) of the daughter molecules. The sister chromatids are then decatenated either prior to completion of replication through decatenation of single-stranded regions (catalysed by a type I topo) or following completion of replication in a reaction catalysed by a type II topo. The data presented here are consistent with such a model whereby Top3^{sp} is required for single-stranded DNA decatenation of newly replicated DNA only following the helicase action of Rqh1. In the

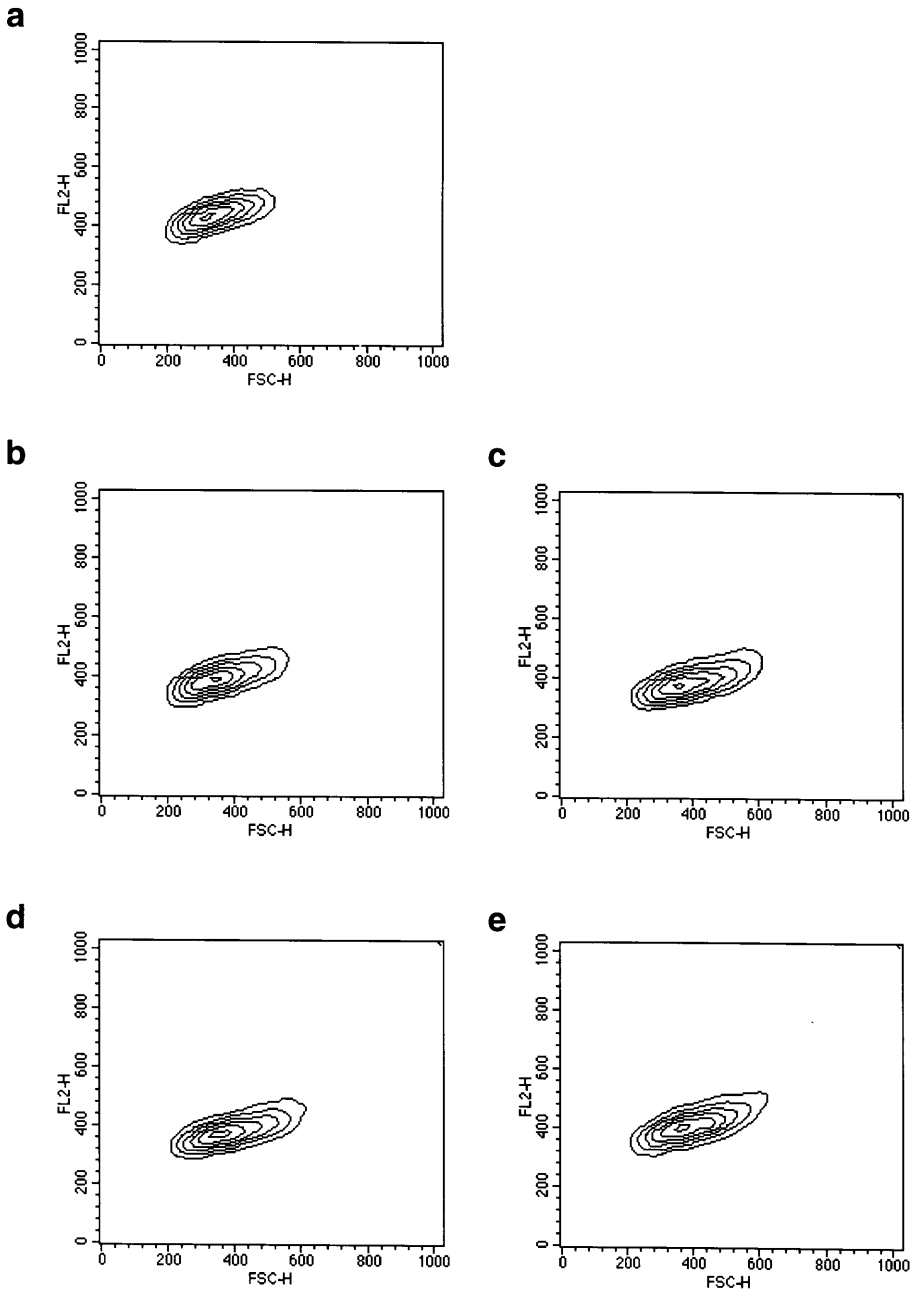

Figure 5. Flow cytometric analysis of the DNA content of wild-type (**a**), *rqh1*::*kanMX6* (**b**), *rqh1-h2* (**c**), *rqh1*::*kanMX6 top3*::*ura4*$^+$ (**d**) and *rqh1-h2 top3*::*kanMX6* (**e**) strains. The vertical axis represents red fluorescence (DNA content) and the horizontal axis forward light scatter (cell size). Note samples isolated from asynchronous, exponentially growing cultures consist predominantly of G_2 cells, as expected of wild-type *S.pombe* cells. The G_2 phase occupies most of the cell cycle and DNA replication occurs close to the time of septation.

absence of both proteins, sister chromatid segregation is catalysed entirely by topo II or through the action of an as yet unidentified alternative DNA decatenase.

Recent biochemical data from Harmon *et al.* (29) have shown that a combination of a RecQ helicase and topo III from *E.coli* can catalyse catenation of two covalently closed DNA duplexes. While this is the reverse of the decatenation required for chromosome segregation, these authors proposed nevertheless that their data are relevant to decatenation reactions, and have provided the first biochemical evidence that the combined actions of helicases and topos are likely to be important during nuclear division.

In summary, we have identified the fission yeast gene encoding the first topo III homologue identified in this

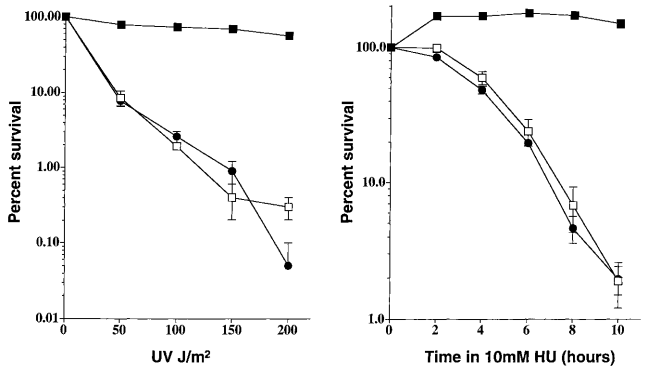

Figure 6. Colony forming assay for wild-type (i.e. *top3*$^+$ *rqh1*$^+$) (filled square), *rqh1*::*kanMX6* (open square) and *rqh1*::*kanMX6 top3*::*ura4*$^+$ (filled circle) strains following exposure to UV light (**left**) or HU (**right**). Points represent the mean of at least three independent determinations. Bars, SE.

organism. *Schizosaccharomyces pombe top3*$^+$ is essential for cell viability through a role in ensuring that nuclear division proceeds faithfully. We have shown that the genetic interaction between genes encoding RecQ helicases and topo III enzymes is conserved from budding yeast to the distantly related fission yeast, strongly suggesting that these two classes of enzymes execute concerted functions in all eukaryotes. This finding has implications for our understanding of the roles of the human RecQ family helicase members encoded by the Bloom's and Werner's syndrome genes in suppressing tumour formation and preventing premature ageing, respectively.

ACKNOWLEDGEMENTS

We thank P. Nurse for yeast strains, J. Bähler for plasmids and members of the ICRF Molecular Oncology Laboratories for useful discussions. Work in the authors' laboratory is supported by the Imperial Cancer Research Fund.

REFERENCES

1. Watt,P.M. and Hickson,I.D. (1994) *Biochem. J.*, **303**, 681–695.
2. Wang,J.C. (1996) *Annu. Rev. Biochem.*, **65**, 635–692.
3. Wallis,J.W., Chrebet,G., Brodsky,G., Rolfe,M. and Rothstein,R. (1989) *Cell*, **58**, 409–419.
4. Gangloff,S., McDonald,J.P., Bendixen,C., Arthur,L. and Rothstein,R. (1994) *Mol. Cell. Biol.*, **14**, 8391–8398.
5. Chakraverty,R.K. and Hickson,I.D. (1999) *Bioessays*, **21**, 286–294.
6. Ellis,N.A., Groden,J., Ye,T.Z., Straughen,J., Lennon,D.J., Ciocci,S., Proytcheva,M. and German,J. (1995) *Cell*, **83**, 655–666.
7. Yu,C., Oshima,J., Fu,Y., Wijsman,E.M., Hisama,F., Alisch,R., Matthews,S., Najura,J., Miki,T., Ouais,S., Martin,G.M., Mulligan,J. and Schellenberg,G.D. (1996) *Science*, **272**, 258–262.
8. German,J. (1995) *Dermatol. Clin.*, **13**, 7–18.
9. Thweatt,R. and Goldstein,S. (1993) *Bioessays*, **15**, 421–426.
10. Epstein,C.J., Martin,G.M., Schultz,A.L. and Motulsky,A.G. (1966) *Medicine*, **45**, 177–221.
11. Chaganti,R.S.K., Schonberg,S. and German,J. (1974) *Proc. Natl Acad. Sci. USA*, **71**, 4508–4512.
12. Fukuchi,K., Martin,G.M. and Monnat,R.J. (1989) *Proc. Natl Acad. Sci. USA*, **86**, 5893–5897.
13. Hanai,R., Caron,P.R. and Wang,J.C. (1996) *Proc. Natl Acad. Sci. USA*, **93**, 3653–3657.
14. Li,W. and Wang,J.C. (1998) *Proc. Natl Acad. Sci. USA*, **95**, 1010–1013.
15. Fritz,E., Elsea,S.H., Patel,P.I. and Meyn,M.S. (1997) *Proc. Natl Acad. Sci. USA*, **94**, 4538–4542.
16. Kawasaki,K., Minoshima,S., Nakato,E., Shibuya,K., Shintani,A., Schmeits,J.L., Wany,J. and Shimizu,N. (1997) *Genome Res.*, **7**, 250–261.
17. Ng,S.W., Liu,Y., Hasselblatt,K.T., Mok,S.C. and Berkowitz,R.S. (1999) *Nucleic Acids Res.*, **27**, 993–1000.
18. Stewart,E., Chapman,C.R., Al-Khodairy,F., Carr,A.M. and Enoch,T. (1997) *EMBO J.*, **16**, 2682–2692.
19. Murray,J.M., Lindsay,H.D., Munday,C.A. and Carr,A.M. (1997) *Mol. Cell. Biol.*, **17**, 6868–6875.
20. Davey,S., Han,C.S., Ramer,S.A., Klassen,J.C., Jacobson,A., Eisenberger,A., Hopkins,K.M., Lieberman,H.B. and Freyer,G.A. (1998) *Mol. Cell. Biol.*, **18**, 2721–2728.
21. Moreno,S., Klar,A. and Nurse,P. (1991) *Methods Enzymol.*, **194**, 795–823.
22. Keeney,J.B. and Boeke,J.D. (1994) *Genetics*, **136**, 849–856.
23. Bahler,J., Wu,J.Q., Longtine,M.S., Shah,N.G., McKenzie,A., Steever,A.B., Wach,A., Philippsen,P. and Pringle,J.R. (1998) *Yeast*, **14**, 943–951.
24. Enoch,T., Carr,A.M. and Nurse,P. (1992) *Genes Dev.*, **6**, 2035–2046.
25. Uemura,T. and Yanagida,M. (1986) *EMBO J.*, **5**, 1003–1010.
26. Uemura,T., Morino,K., Uzawa,S., Shiozaki,K. and Yanagida,M. (1987) *Nucleic Acids Res.*, **15**, 9727–9739.
27. Watt,P.M., Louis,E.J., Borts,R.H. and Hickson,I.D. (1995) *Cell*, **81**, 253–260.
28. Rothstein,R. and Gangloff,S. (1995) *Genome Res.*, **5**, 421–426.
29. Harmon,F.G., DiGate,R.J. and Kowalczykowski,S.C. (1999) *Mol. Cell*, **3**, 1–20.